On the use of Doppler-shift estimation for simultaneous underwater acoustic localization and communication

C. Aubry, Pierre-Jean Bouvet, A. Pottier, Y. Auffret, Philippe Forjonel

On the use of Doppler-shift estimation for simultaneous underwater acoustic localization and communication

C. Aubry, P. Forjonel, P.-J. Bouvet, A. Pottier and Y. Auffret
L@bisen, SEANERGY lab
ISEN Brest YNCREA Ouest
Brest, France
Email: philippe.forjonel@isen-ouest.yncrea.fr

***Abstract*—Due to the relative low propagation speed of acoustic waves in underwater medium, Underwater Acoustic (UWA) communication is severely impacted by Doppler shift effect especially as the transmission link is related to a system in motion like an Autonomous Underwater Vehicle (AUV). Usually, motion-induced Doppler-shift needs to be estimated and compensated at the UWA receiver side in order to retrieve data. This estimation also provides an information on transmitter/receiver relative speed that is valuable for an underwater mobile like an AUV to perform underwater localization and navigation. In this paper, we consider a reference anchor transmitting UWA data to an AUV in operation. The latter uses UWA communication decoding process to estimate both range and relative speed with respect to the reference point in order to improve its navigation via a conventional Kalman filtering. Simulation results on a shallow water channel demonstrate the Doppler shift estimation to provide substantial enhancement of the underwater localization with respect to a range-only approach.**

I. Introduction and motivations

Conventional aerial communication scheme (like cellular network) and localization system (like GPS) cannot be used underwater and acoustic based approach are mostly preferred. However, the relative low celerity of the acoustic waves poses significant challenge for both data communication [1] and underwater target localization and tracking [2].

Among all detrimental effects of the UWA channel for data transmission, the Doppler scaling effect is perhaps the worst one and requires at the decoding side, especially in the case of coherent modulation, a specific pre-processing stage including an estimation and compensation of such effect [3]. The Doppler scale is influenced by motion of the transmitter/receiver or any reflection points in the channel that leads to time-varying path propagation delay. This includes unintentional movement like drifting, see surface motion and vehicular motion between transmitter and receiver [4], [5].

On the other hand, to compute its location, an AUV uses both proprioceptive (inertial sensors, compass) and exteroceptive (SONAR, video camera, GPS at surface,...) information. A good knowledge of the vehicular motion is an important component to estimate the vehicle position. Such information can be efficiently provided by a Doppler Velocity Log (DVL) sensor but comes with a substantial hardware cost. A cheaper alternative of the DVL is the use of Doppler shift estimations that are measured opportunistically by the UWA communication links as shown in [6]–[8].

In this paper we consider an AUV following a planned route and receiving cyclically UWA data from a reference fixed beacon. We implement an algorithm that uses both range and Doppler shift estimation provided by the UWA communication demodulator in order to improve AUV localization algorithm and thus reduce AUV navigation error. The originality of the paper lies in the complete simulation of UWA communication link and in the study of its impact on the localization algorithm.

II. UWA communication model

A. Transmitted signal

Data transmission is carried out frame by frame. Each frame starts with pilot symbols belonging to a Pseudo-Noise (PN) sequence that are used for synchronization and channel estimation. The remaining of frame contains N_d data Phase Shift Keying (PSK) symbols, generated with a Bit-Interleaved and Coded Modulation (BICM) scheme, that carry the useful information. Within the frame, the complex symbol at index $k \in [0, N_p + N_d - 1]$ is noted $x[k]$. Each symbol is then pulse-shaped using a Square Root Raised Cosine (SRRC) filter with roll-off factor β and symbol duration T, and finally transposed around center frequency f_0.

In order to estimate accurately the Doppler shift at the receive side, an out-of-band pure tone signal around frequency f_{pt} is added to the useful signal [9] such that, for a given frame, the final passband signal transmitted through transducer is expressed as:

$$s(t) = \Re\left[e^{j2\pi f_{pt}t} + \sum_{k=0}^{N_p+N_d-1} x[k]g_T\big(t-kT\big)e^{j2\pi f_0 t}\right] \quad (1)$$

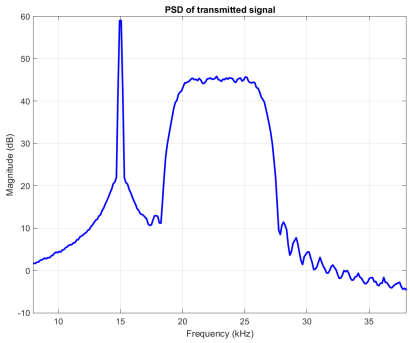

Fig. 1. PSD of transmitted UWA communication signal.

where $g_T(t)$ represents the impulse response of SRRC filter. The Power Spectral Density (PSD) of the transmitted pass-band signal is depicted in figure 1.

B. UWA channel model

The UWA channel is modeled by the following time-varying transfer function originally introduced in [4]:

$$H(f,t) = \bar{H}_0(f) \sum_p h_p \gamma_p(f,t) e^{-j2\pi f \tau_p(t)} \tag{2}$$

where $\bar{H}_0(f)$ is the transfer function of direct path (taking into account both absorption and path loss), h_p is the relative path gain assumed constant for a frame, $\gamma_p(f,t)$ represents the scattering coefficient modeled by a complex-valued Gaussian processes whose statistics reflects the time coherence of the channel and $\tau_p(t)$ the path delays which vary in time according to the relative motion $v_r(t)$ between transmitter and receiver:

$$\tau_p(t) = \bar{\tau}_p - \int_0^t \frac{v_r(t)}{c_w} dt \tag{3}$$

where $\bar{\tau}_p$ is the nominal path delay and c_w is the speed of sound in water. Whereas the time variation due to the scattering coefficient $\gamma_p(f,t)$ leads to Doppler spread, the time variation of the path delay leads to fast phase rotation of $-j2\pi f \tau_p(t)$ known as motion induced Doppler frequency shift. For simplicity, the relative velocity is assumed identical for each path and can be decomposed as follows [4]:

$$v_r(t) = v_{rd}(t) + v_{rv}(t) + v_{rs}(t) \tag{4}$$

where $v_{rd}(t)$ denotes unintentional transmitter-receiver motion (like drifting), $v_{rv}(t)$ is the vehicular motion and $v_{rs}(t)$ represents the surface motion due to waves.

Finally, the ambient noise is modeled by a white Gaussian process with a power depending on the transmit frequency bandwidth [1].

C. Doppler-shift estimation and data decoding

Let us now define $\tilde{r}_{pt}(t)$ the baseband received signal centered around f_{pt} corresponding to received pure-tone pilot signal. Due to the narrow-band nature of the pure tone signal, an estimation of the instantaneous Doppler shift can be extracted from the phase derivative of $\tilde{r}_{pt}(t)$. In practice, such estimation is easily obtained by computing the phase rotation from two successive samples. From (2) and (3), an estimation of the relative velocity at sampling time kT can be formed as:

$$\hat{v}_r(kT) = \frac{c_w}{2\pi T f_{pt}} \arg\Big(\tilde{r}_{pt}(kT)\tilde{r}^*_{pt}\big((k-1)T\big)\Big) \tag{5}$$

Motion induced Doppler shift is usually removed from the received useful baseband signal $\tilde{r}(t)$ via re-sampling and phase compensation [3]:

$$y[k] = \tilde{r}(\hat{t}_k)\exp(-j\hat{\phi}_k) \tag{6}$$

where $\hat{t}_k$ and $\hat{\phi}_k$ are updated dynamically from the instantaneous relative velocity estimation:

$$\begin{cases} \hat{t}_k = \hat{t}_{k-1} + T\Big(1 - \frac{\hat{v}_r(kT)}{c_w}\Big) \\ \hat{\phi}_k = \hat{\phi}_{k-1} + 2\pi f_0 T \frac{\hat{v}_r(kT)}{c_w} \end{cases} \tag{7}$$

Data decoding is finally performed from signal $y[k]$ by using advanced equalization processing and channel decoding. In our case we consider a Single Input Multiple Output (SIMO) turbo-equalizer with residual phase compensation as described in [10].

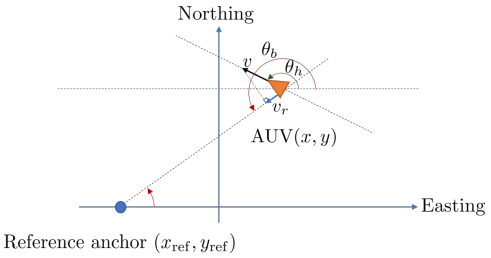

Fig. 2. AUV position with respect to reference anchor.

III. Underwater navigation and localization

A. State space model

The AUV has a position (x,y), a velocity v and a heading angle θ_h. The heading angle of the robot is considered to be measured accurately (or returned from an Inertial Measurement Unit (IMU), [11]). A reference anchor is assumed fixed with known position $(x_{\text{ref}}, y_{\text{ref}})$. As described in figure 2, the bearing angle θ_b of the reference viewed by the AUV is:

$$\theta_b = \text{atan2}\Big(y - y_{\text{ref}}, x - x_{\text{ref}}\Big) + \pi \tag{8}$$

The relative vehicular velocity can be computed as:

$$v_{rv} = v\cos(\theta_b - \theta_h) \tag{9}$$

The AUV to be considered in this simulation is modeled by classical cart robot controlled by angular velocity and acceleration. The AUV is then regulated via a feedback linearization method on a known trajectory.

B. Kalman filter

A classical approach in robot localization is the use of probabilistic state estimation [12]. The widely used are Bayesian filters: Kalman filter and Particle filter. On this paper, we will focus on a Kalman filter [13] to estimate robot position and speed among the trajectory in a state vector $\mathbf{z} = (\hat{x}, \hat{y}, \hat{v})^T$. We can write the model to be used by the Kalman filter as a linear one [14]:

$$\frac{d}{dt}\begin{pmatrix}\hat{x}\\ \hat{y}\\ \hat{v}\end{pmatrix} = \begin{pmatrix}0 & 0 & \cos\theta_h\\ 0 & 0 & \sin\theta_h\\ 0 & 0 & 0\end{pmatrix}\begin{pmatrix}\hat{x}\\ \hat{y}\\ \hat{v}\end{pmatrix} + \begin{pmatrix}0\\ 0\\ 1\end{pmatrix} u_2 \qquad (10)$$

where u_2 is the acceleration command. Measurements taken into account in the Kalman filter are the squared distance to the anchor and vehicular relative speed.

IV. Simulation results

A. System parameters

The reference anchor is positioned on the x-axis at 150 m west from the origin. Every 10 seconds, the reference anchor sends an UWA message to the AUV by using a waveform centered on $f_0 = 23$ kHz with a symbol bandwidth of $B = 1/T = 6.4$ kHz and a SRRC roll-off ratio of $\beta = 0.4$. Each frame carries $N_d = 2518$ data symbols and starts with $N_p = 150$ pilots yielding to a message duration of 416.9 ms. The BICM encoder employs an half-rate 64-state convolutionnal encoder and 4-state PSK constellation leading to a net bitrate of 6.04 kBits/s. The pure tone signal is set outside the useful band with $f_{pt} = 15$ kHz.

The UWA channel is assumed to be shallow water with a constant depth of 10 m. The anchor transmitter and the AUV receiver are positioned at 1 m depth. The relative surface velocity is assumed negligible and relative drift velocity $v_{rd}(t)$ oscillates in the range of ± 0.1 m/s. The statistical properties of the scattering coefficients $\gamma_p(f,t)$ are set according to [4] leading to an effective Doppler spread per channel path varying from 0 to 3 Hz . The signal level at the transmitter is set such that the Signal-to-Noise Ratio (SNR) be equal to 15 dB at the maximum communication range. At the receiver side, the AUV employs 4 receive streams that are fed to the SIMO decoder.

The AUV is regulated via a feedback linearization on a Lemniscate trajectory described by the following equation:

$$\begin{cases} x_d = a\sin(f_1 t)/(1+\cos(f_1 t)^2) \\ y_d = a\sin(f_1 t)\cos(f_1 t)/(1+\cos(f_1 t)^2) \end{cases} \qquad (11)$$

with $a = 500$ m and $f_1 = 0.0045$ Hz, the duration of the mission is 1350 s. Those parameters are estimated to get a pertinent speed of some meters per seconds. Kalman filter is configured with a covariance matrix for the model noise defined by $0.1 \cdot \mathbf{I}$. The observation noise covariance matrix is filled at each received communication with variances of each measurements directly computed during UWA channel estimation and decoding processes.

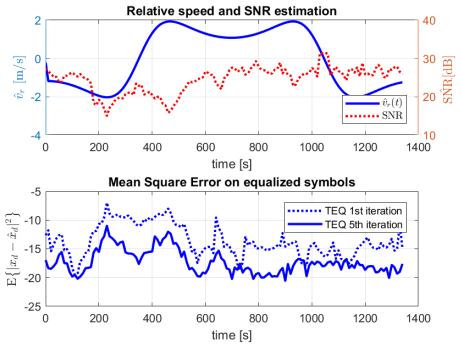

Fig. 3. UWA communication metrics and performance.

B. UWA communication performance

Figure 3 provides performance metrics of the UWA communication link for the first 135 messages transmit from the anchor to the AUV that corresponds to an effective time of 1350 seconds of trajectory simulation. For each message, the simulation is run 10 times in order to average the channel statistics. On the upper plot, the estimated relative velocity and SNR are drawn as a function of the navigation time. Depending on the AUV position, the relative velocity estimate vary in the range of ± 2 m/s. The estimation error is mainly due to drifting effect and the associated standard deviation remains below 0.1 m/s. In the lower plot, the Mean-Square Error (MSE) between the transmitted 4-PSK symbols and equalized ones is carried out for the 1st and 5th iteration of SIMO turbo-equalizer. As expected, the MSE is inversely proportional to the channel SNR, and remains below -12 dB after 5 iterations of the receiver that ensures an error free transmission for all transmitted frames after soft Viterbi decoding.

C. Localization performance

Figure 4 shows results of a simulation where the robot is regulated on a trajectory and where Kalman filter is used to estimate the position of the robot with a measurement of speed from UWA communication. No range is taken into account in this experiment. We can see on this plot that the size of the 90% confidence ellipsoid grows nearly in a linear form, which is expected as speed is a proprioceptive information. This information can be read with blue curves from figure 5 which shows on top the positioning error (i.e. distance from estimation to truth) and on the bottom the Root Mean Square Error (RMSE) equal to the norm of the covariance matrix associated with the position estimation of the Kalman filter.

The RMSE of the experiment with only speed measurement can be split in 3 linear parts, each part separated with peaks that are caused by the orthogonality of the trajectory from anchor to AUV with respect to AUV heading. We see on the top of figure 5 that positioning error also grows "linearly" which is represented on figure 4 by center of ellipsoids

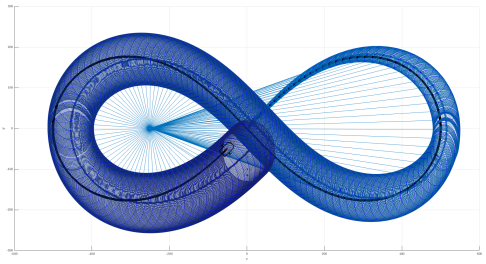

Fig. 4. Trajectory simulation of the AUV localized by a Kalman filter with speed measurement. Solid line represents an UWA transmission.

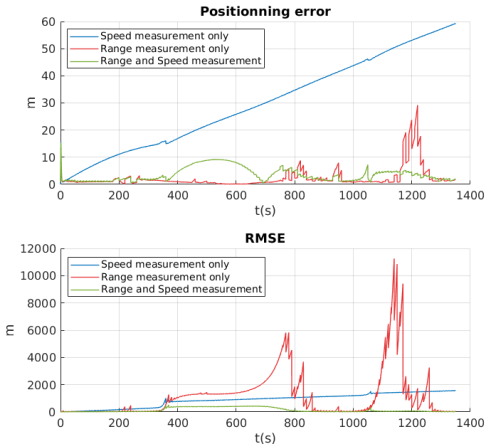

Fig. 5. Characterization of localization error and error dispersion.

trajectory that not fit with true trajectory.

Figure 7 shows another simulation where the Kalman filter also takes as an observation range measurement and associated variance extracted from channel estimation process of UWA channel decoding. RMSE and positioning error are also depicted in figure 5. We can see that if positioning error is mainly higher when compared to the same error without speed measurement, RMSE is significantly lower which is a real improvement. The peaks on the range only RMSE curve are explained by the fact that for this measurement, the AUV is nearly heading to the anchor and the variance associated is very high. This phenomena is significantly reduced with speed measurement. A point that is not clearly shown on figure 5 is the fact that the ellipses are oriented, this could be seen when plotting RMSE among axes of the plan.

V. Conclusion

This paper presented results on the impact of the use of speed measurement in a localization algorithm where dead-reckoning is corrected with range measurement from a moving AUV to a fixed anchor. The Doppler effect induced in communication from the anchor to the AUV induced by the movement of the AUV allows us to measure the speed of the robot while communicating and ranging. Those results show that while error in distance measurements can grow when the AUV is facing the anchor (increasing variance of

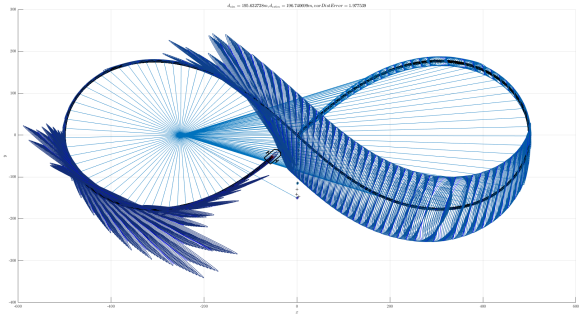

Fig. 6. Trajectory simulation of the AUV localized by a Kalman filter with range measurement. Solid line represents an UWA transmission.

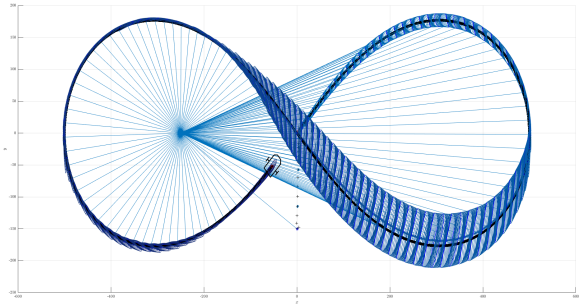

Fig. 7. Trajectory simulation of the AUV localized by a Kalman filter with speed and range measurement. Solid line represents an UWA transmission.

the measure), speed measurements can prevent this error to grow too fast. In another hand, navigating in dead-reckoning with speed measurement only can induce a drift in the position estimation that can be corrected by adding range measurement. Future works will include noise in the model, a comparison with nonlinear versions of Kalman filter (UKF/EKF) as well as validation on sea experiments.

References

[1] M. Stojanovic and P.-P. J. Beaujean, "Acoustic Communication," in *Springer Handbook of Ocean Engineering*, M. R. Dhanak and N. I. Xiros, Eds. Springer International Publishing, 2016, pp. 359–386.

[2] H.-P. Tan, R. Diamant, W. K. G. Seah, and M. Waldmeyer, "A survey of techniques and challenges in underwater localization," *Ocean Engineering*, vol. 38, no. 14, pp. 1663–1676, Oct. 2011. [Online]. Available: http://www.sciencedirect.com/science/article/pii/S0029801811001624

[3] T. H. Eggen, A. B. Baggeroer, and J. C. Preisig, "Communication over Doppler spread channels. Part I: Channel and receiver presentation," *IEEE Journal of Oceanic Engineering*, vol. 25, no. 1, pp. 62–71, Jan. 2000.

[4] P. Qarabaqi and M. Stojanovic, "Statistical Characterization and Computationally Efficient Modeling of a Class of Underwater Acoustic Communication Channels," *IEEE Journal of Oceanic Engineering*, vol. 38, no. 4, pp. 701–717, Oct. 2013.

[5] S. Pinson and C. W. Holland, "Relative velocity measurement from the spectral phase of a match-filtered linear frequency modulated pulse," *The Journal of the Acoustical Society of America*, vol. 140, no. 2, pp. EL191–EL196, 2016.

[6] R. Diamant, L. M. Wolff, and L. Lampe, "Location Tracking of Ocean-Current-Related Underwater Drifting Nodes Using Doppler Shift Measurements," *IEEE Journal of Oceanic Engineering*, vol. 40, no. 4, pp. 887–902, Oct. 2015.

[7] P. Carroll, K. Domrese, H. Zhou, S. Zhou, and P. Willett, "Doppler-aided localization of mobile nodes in an underwater distributed antenna system," *Physical Communication*, vol. 18, pp. 49–59, Mar.

2016. [Online]. Available: http://www.sciencedirect.com/science/article/pii/S1874490715000439

[8] O. Pallares, P. J. Bouvet, and J. d. Rio, "TS-MUWSN: Time Synchronization for Mobile Underwater Sensor Networks," *IEEE Journal of Oceanic Engineering*, vol. 41, no. 4, pp. 763–775, Oct. 2016.

[9] P. Kathiroli, P. P. J. Beaujean, and N. Xiros, "Source speed estimation using a pilot tone in a high frequency acoustic modem," in *OCEANS'11 MTS/IEEE KONA*, Sep. 2011, pp. 1–8.

[10] P. J. Bouvet, Y. Auffret, D. Munck, A. Pottier, G. Janvresse, Y. Eustache, P. Tessot, and R. Bourdon, "Experimentation of MIMO underwater acoustic communication in shallow water channel," in *OCEANS 2017 IEEE - Aberdeen*, Jun. 2017, pp. 1–8.

[11] C. Aubry, R. Desmare, and L. Jaulin, "Loop detection of mobile robots using interval analysis," *Automatica*, vol. 49, no. 2, pp. 463–470, 2013.

[12] S. Thrun, W. Bugard, and D. Fox, *Probabilistic Robotics*. Cambridge, M.A.: MIT Press, 2005.

[13] R. E. Kalman, "A new approach to linear filtering and prediction problems," *Transactions of the AMSE, Part D, Journal of Basic Engineering*, vol. 82, pp. 35–45, 1960.

[14] L. Jaulin, M. Kieffer, O. Didrit, and E. Walter, *Applied Interval Analysis*. Springer, 2001.